NEAR-NOZZLE LDA/PDA MEASUREMENTS OF A GDI SPRAY AND THEIR ANALYSIS TO QUANTIFY LIQUID BREAKUP AND ATOMIZATION MECHANISMS

G. Wigley[1], M. Goodwin[1], G. Pitcher[2] and D. Blondell[3]

[1]**Aeronautical & Automotive Engineering Department, Loughborough University, Leicestershire, LE 11 3TU, UK**
[2]**Lotus Engineering, Hethel, Norwich, NR14 8EZ, UK**
[3]**Dantec Dynamics A/S, DK-2740 Skovlunde, Denmark**

Abstract

The paper describes the relationship between Laser Doppler velocity data and size-class discriminated Phase Doppler velocity data for the temporal and spatial development of the spray produced by a gasoline pressure swirl injector. The data presented cover the region from the nozzle orifice to 5 mm downstream where the spray is optically dense and only partially atomized. The analysis method allows a much deeper understanding of the liquid sheet break up and atomization processes occurring in the spray to be presented.

1. Introduction

Velocity measurements obtained by the Laser and Phase Doppler technique can differ significantly in partially atomized sprays [1]. This has been attributed to the fact that each instrument responds differently to the light scatterers contained in the spray. In principle, the Laser Doppler, LD, system will respond faithfully to any light scatterer passing through the measurement volume irrespective of its form, whereas, the Phase Doppler, PD system should only respond to light scatterers in droplet form. The PD system responds to droplets, not only spherical droplets, but elliptical droplets can also be validated, [1] and [2]. In the partially atomized regions of a spray produced by a single fluid injector the velocity data recorded by an LD experiment have been seen to be higher than that determined by a PD experiment. The converse is true in the partially atomized spray regions of an air blast, dual fluid injector. In both cases, the LD data have been used as a representative measure of the velocity of all liquid forms, i.e. liquid sheets, jets, filaments, ligaments and droplets, while the PD data is representative of the droplets or the atomized content of the spray.

This paper describes a simultaneous LD/PD investigation, supported by single shot CCD imaging, of the spray produced in the near nozzle region of a pressure-swirl Gasoline Direct Injection, GDI, injector. A detailed analysis of the spray images and measured liquid flow velocity and the droplet velocities and size is performed in order to quantify the liquid break up and atomization mechanisms.

2. Instrumentation and Experimental Technique

2.1 Injector and injection system

The Mitsubishi GDI pressure swirl injector was used in this study. The swirl generator and nozzle assembly are shown in Figure 1. The six tangential fuel channels are 0.25 mm high and 0.61 mm wide and feed fuel through the 96^0 cone of the needle seat into the nozzle orifice of diameter 0.90 mm. The swirling annular flow structure generated inside an optical nozzle fitted with the swirl generator of a Mitsubishi GDI injector has been imaged, [3]. An air vortex is formed along the entire length of the nozzle axis with an annulus of liquid fuel firmly attached to the wall. Other optical nozzle studies, [4], confirm this internal swirling nozzle flow but furthermore indicates that the external flow is a hollow cone sheet which breaks up at a very short distance downstream of the injector. This break up length is typically of the order of the nozzle orifice diameter and the maximum diameter of the primary droplets is typical of the sheet thickness at that location. The injector was operated at 50 bar fuel pressure with a fuel solenoid opening time of 0.85 ms corresponding to a fuel delivery of 11.0 mg per injection into ambient air.

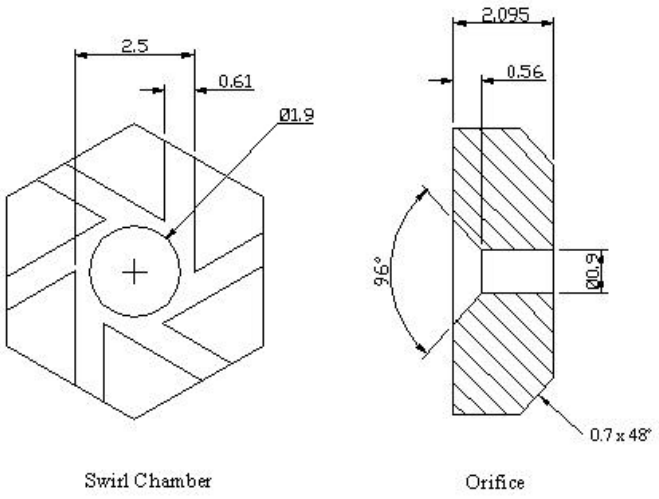

Figure 1 Pressure swirl injector

2.2 Imaging system

For this study a back-lit illumination scheme was adopted with a small degree of supplementary front lighting applied. Two EG&G MVS 7020 Xenon flash units were used. One was coupled to a Fostec fibre optic panel to provide a uniform background light intensity against which the spray was imaged, while the other, coupled to a normal Fostec fibre optic cable, projected the second flash onto the front of the spray. The single-shot images were digitally recorded with a PCO Sensicam Fast Shutter CCD camera equipped with a Nikon 55 mm focal length macro lens. The image plane was on the spray axis, therefore, only the outer edges of the spray cone were focussed correctly. It provided an image size of 21 by 17 mm, represented by 1280 by 1024 pixels, and a depth of field of approximately 3 mm. The camera shutter speed was set to 0.5 micro-second with a frame rate of 8 Hz. The injector control unit provided an electronic trigger, referenced to the opening pulse of the injector solenoid, which, through a variable delay unit, controlled both the flash and image capture time.

2.3 The Phase Doppler system

The design and construction of the two component high power, high spatial resolution LD/PD transmission system has been well documented, [5]. The transmitter sections were configured with the 488 and 514 nm laser beam wavelengths for the radial and axial velocity components. With 50 mm beam pair separations for each wavelength at the 300 mm focal length focussing lens, coincident measurement volumes of diameters of 42 and 45 microns were produced with laser powers of 120 and 250 milli-watts per beam respectively. The standard Dantec 57X10 receiver optical system was positioned at a scattering angle of 70^0 while the aperture micrometer setting was set to 0.5 mm. This optical configuration resulted in an effective measurement volume length of 0.11 mm, a maximum drop size measurement capability of 100 microns and a phase/size measurement resolution of 6.60 degrees/micron.

Two different generations of Dantec PDA signal processors were used in this work, the Enhanced 58N50 Covariance processor and the latest BSA-P80 processor. However, the Covariance processor was only configured for two component velocity measurements as the signal phase/delay calibration signals were specific to the BSA P80/receiver combination, [6]. Throughout the paper the droplet velocity and size data obtained by the BSA P80 and the liquid + droplet velocity data obtained by the Covariance processor are referred to as the PD and LD data respectively.

The LD/PD measurement grid started on the nozzle geometric axis at Z = 0.5 mm and extended down to Z = 5.0 mm below the nozzle and reached out to 1.0 and 4.0 mm radially respectively. At each measurement position 20,000 validated data samples were attempted or an elapsed time of 125 seconds was reached i.e. 1000 injections. Invariably the Covariance processor collected the 20,000 velocity-only samples in a shorter time than the BSA P80 processor, especially on the inside edge of the spray cone.

Data analysis was performed in two stages. In stage 1, both the PD and LD data were time bin averaged, over sector sizes of 40 micro-seconds, to produce comprehensive time varying mean profiles of axial and radial velocity, dropsize and sample number. In stage 2, a size-class discrimination was applied to the PD velocity data, before the time-bin averaging process was performed, to produce comprehensive time varying mean profiles of axial and radial velocity for distinct size-classes. Three size-classes of 0 to 4, 8 to 16 and 16 to 64 microns were then chosen for presentation as being representative of how the different dropsize classes determined the spray characteristics.

3. Results and discussion

The main stages of the spray cone development are shown by four CCD single shot images in Figure 2. The image times are relative to the electronic trigger to the injector and fuel first appears at the nozzle orifice at 0.42 ms.. Overlaid onto each image is a 1 mm square grid and the light transmission profiles for the axial planes Z = 1 to 5 mm in 1 mm steps. The minimum light transmission for each profile is aligned with the relevant axial plane. A recent review of imaging methods for diesel sprays, [7], stated that, with a direct or shadowgraph imaging method, it was difficult to obtain information related to the internal structure of the dense core region due to high obscuration and line of sight integration. However, in the work performed here, the imaging analysis was used solely to identify where the dense regions in the spray periphery were as regards the core, for the pre-swirl spray and the cone, for the developing spray.

The pre-swirl spray image at 0.56 ms shows that the spray tip has penetrated to Z = 10 mm and large liquid ligaments exist below Z = 5 mm. There is a high intensity of the reflected forward lighting from the spray core for the first 2 mm downstream from the nozzle. An analysis of the LD and PD data across the pre-swirl spray periphery shows that the liquid + droplet velocity and sample number can be double the droplet velocity and sample number indicating that, while fuel break-up is effective, atomization is not. The bright 'spots' on each image are due to large sporadic drops on the spray periphery reflecting the forward lighting.

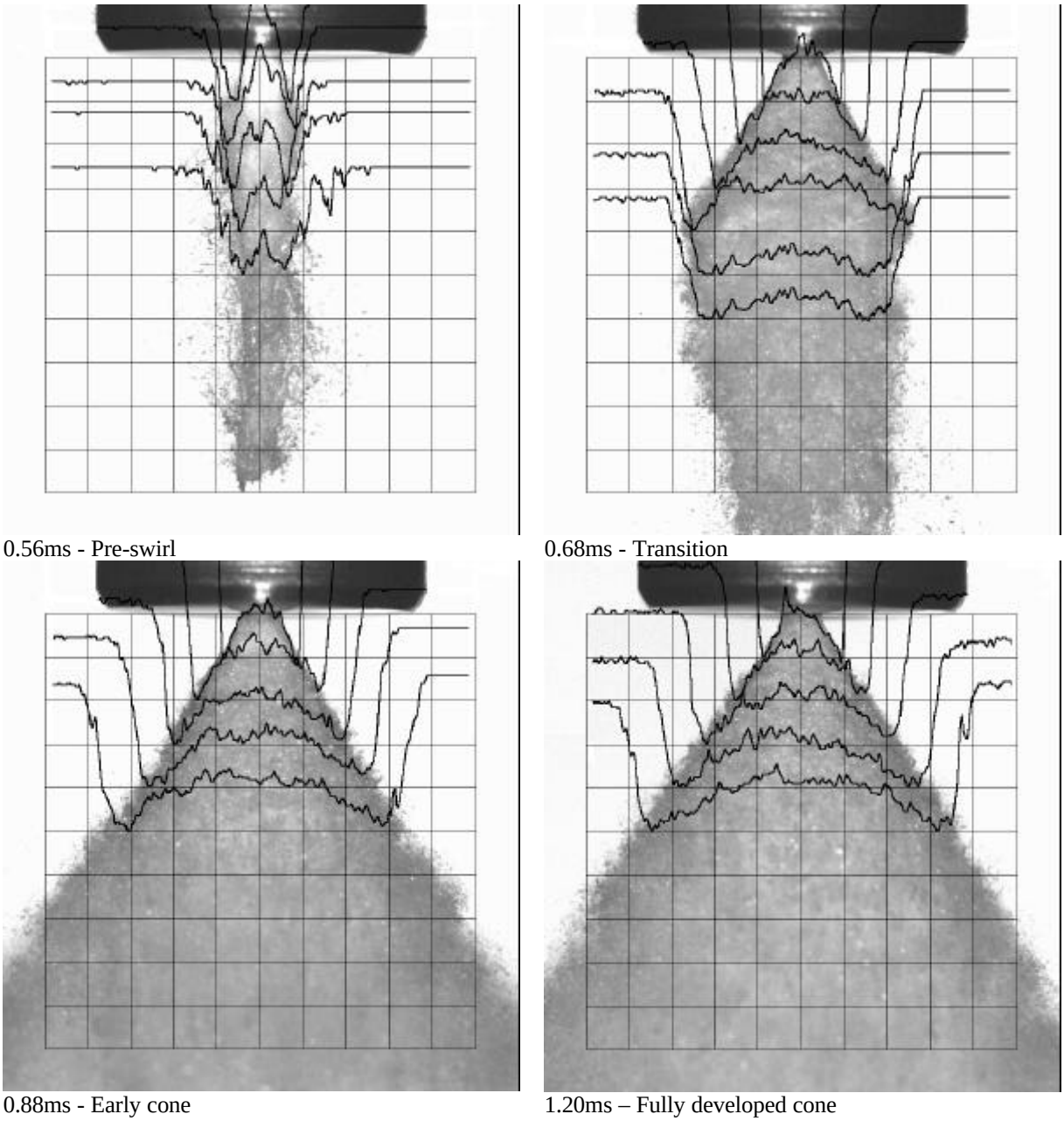

0.56ms - Pre-swirl

0.68ms - Transition

0.88ms - Early cone

1.20ms – Fully developed cone

Figure 2 Images at four stages of the spray development

The radial profiles of the axial and radial velocity components for this pre-swirl spray are shown uppermost in Figure 3. The general form for both are as expected for a 'free jet' with a peak axial and zero radial velocity on the spray axis. What is a little surprising, at first sight, is that the axial velocity on the axis appears to increase with distance downstream from the nozzle. The answer to this lies both with the nature of the axial variation in the intensity profiles and the velocity profiles for the preceding two time bins at 0.48 and 0.52 ms.

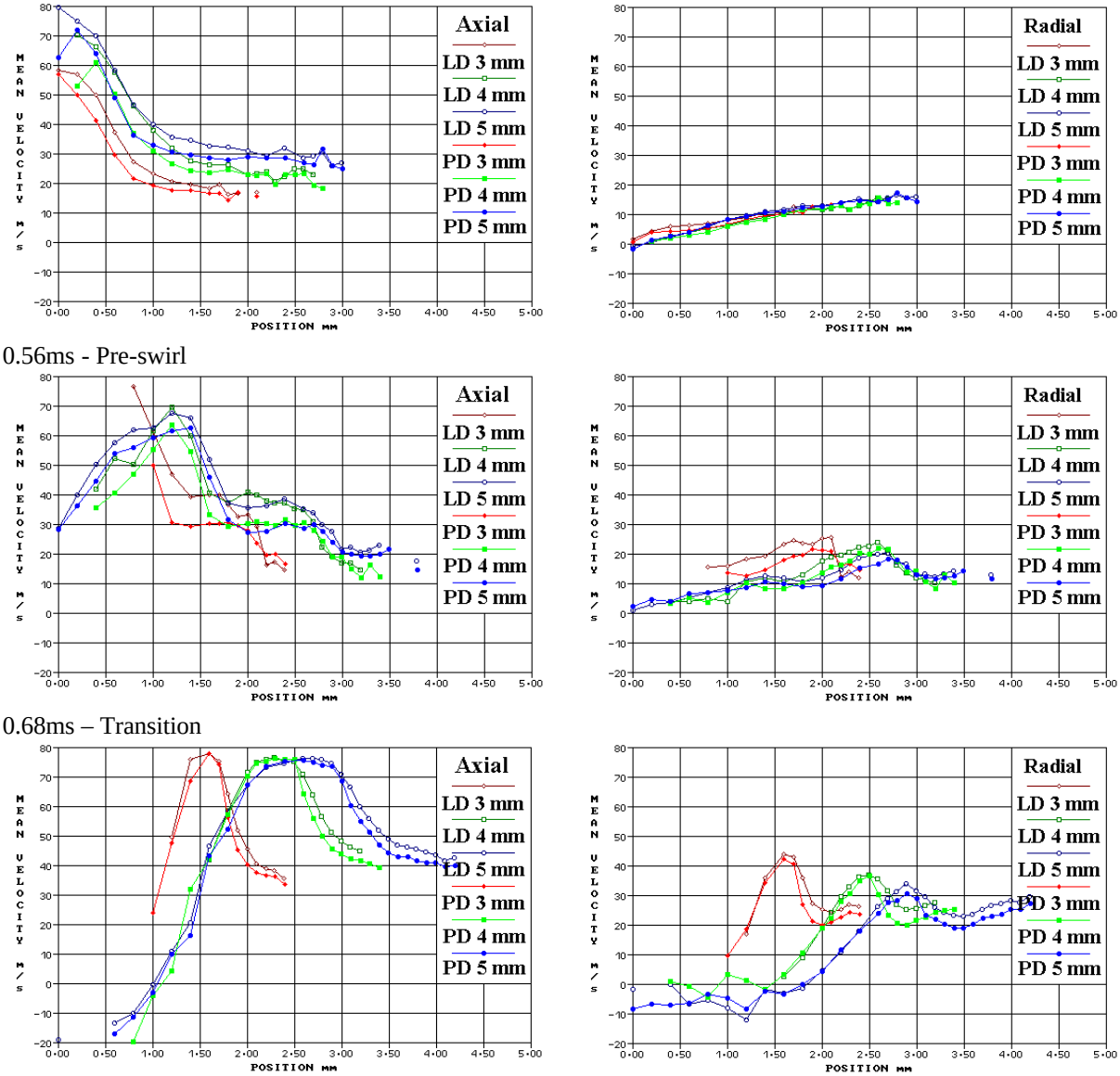

0.56ms - Pre-swirl

0.68ms – Transition

1.20ms – Fully developed cone

Figure 3 Axial and radial velocity profiles for the LD and PD data sets

The mean intensity profiles show the minimum level of light transmission at Z = 2 mm is, at R = 1.8 mm, at a greater radial location than in the other planes. This infers that the external swirling flow has started to affect the distribution of fuel inside the spray core. Furthermore, the axial velocity for the time bin centred on 0.48 ms does show the same peak axial velocity, of approximately 72 m/s, occurring along the length of the spray axis between Z = 1 and 5 mm. The conclusion here is that the pre-swirl spray comprises of a pure jet flow from 0.42 to 0.48 ms. As the swirl momentum increases fuel is transferred radially outwards and a low pressure zone on the spray axis is created. This transition reaches Z = 3 mm by 0.56 ms.

Two profiles, for each velocity component, representing the liquid + droplet and droplet data are also shown in Figure 3 for the axial planes of 3, 4 and 5 mm. In general, the LD velocity magnitudes are greater than the equivalent PD velocities in those regions affected by high shear forces and are equal where small time scales and size classes dominate.

Consider, first, the velocity plots for the pre-swirl spray. For Z = 4 and 5 mm, the axial velocity profiles for the spray core are very similar, for both the LD and PD data, out to R = 1 mm. Beyond this, the LD data exhibit a higher velocity when compared with the PD data. However, at Z = 3 mm there are significant differences between the data sets across the whole

spray radius. In the spray core the droplets and liquid are travelling at the same velocity but this state is altered when the droplets interact with the shear gradients generated in the spray periphery and by the transition from the core to cone at Z = 3 mm. The radial velocity components for the LD and PD data sets are virtually identical for the pre-swirl spray.

For the transition phase the differences in the LD and PD axial velocities for Z = 4 and 5 mm in the spray periphery, R > 1.8 mm, are of a comparable magnitude to those in the pre-swirl spray. However, large differences, up to 5 m/s, are to be found between the two across the central regions in the developing hollow spray cone. This again, is not seen in the data for radial velocity which show that differences between the data sets develop only in the spray periphery. The LD and PD velocity data for the Z = 3 mm plane again show substantial differences, of up to 10 m/s, across the width of the spray. Measurements between the spray axis and R = 1 mm were not made, by either the LD or the PD technique, due to the optically dense nature of the partially atomized spray and, in part, to the limited data acquisition time.

The LD and PD profiles for all three axial planes show consistent trends for the fully developed spray cone. The LD and PD velocity data are the same inside the hollow cone but after the velocity profiles peak, in the cone itself, the PD velocity data is always less than that shown by the LD data, by up to 5 m/s in both the axial and radial velocity components. At Z = 3 mm the peak in both the axial and radial profiles occur R = 1.6 mm. At Z = 4 and 5 mm the peak in the axial velocity occurs at a slightly smaller radius than for the radial velocity component, e.g. R = 2.6 and 2.9 mm respectively at Z = 5 mm.

To analyse these phenomena the PD velocity profiles were re-calculated according to size-class. Velocity data for three size-classes, 0 to 4, 8 to 16 and 16 to 64 microns have been chosen for presentation. The arithmetic mean droplet diameter, D_{10}, profiles for the three different phases of the spray development are shown in the left hand column of Figure 4. In the right hand column are the axial and radial velocity data, according to size-class discrimination, together with the equivalent LD velocity data for the axial plane Z = 5 mm.

The D_{10} dropsize profiles for Z = 3,4 and 5 mm and three phases of the spray development will be discussed first. The dropsize profiles for the pre-swirl phase of the spray clearly shows that the largest mean diameters, of up to 30 microns, are to be found on the spray axis. All three profiles then show a minimum, between 6 and 7 microns, for the radial location of 0.8 mm before doubling in magnitude in the spray periphery. In this spray, a high recorded mean dropsize is indicative of the presence of a wide range of sizes.

As the annular liquid film from the injector orifice swirls radially outwards so does the peak in the dropsize profiles. This is accompanied by a significant reduction in the dropsize along the spray axis of the hollow cone as only the smallest of size-classes can be expected to remain in this low pressure region. Relatively small dropsizes and therefore range of sizes is to be found during the transition phase at 0.68 ms suggesting that atomization is more effective due to the high shear generated as the liquid fuel rapidly expands radially.

With the cone fully established at 1.20 ms the dropsize profiles again show distinct peaks at all three axial planes. Mean droplet diameters of less than 5 microns occupy the hollow cone of the spray. There is a maxima in the mean droplet diameter profiles of 22 microns at Z = 3 mm which then decreases to 18 and 16 microns at Z = 4 and 5 mm respectively. The mean droplet diameters then decrease but an inflection point is found as the mean droplet diameters then increase again steadily out into the spray periphery.

A comparison of the LD and the size-class PD velocity data in Figure 4 shows a ‘best fit’ to the size-class profiles of 8 to 16 microns. This supports the assumption that the LD system responds to all liquid forms. Since the large fuel elements and droplets will maintain their high momentum, the LD data will always exceed the PD velocity data where the spray is partially atomized or a wide range of sizes is present.

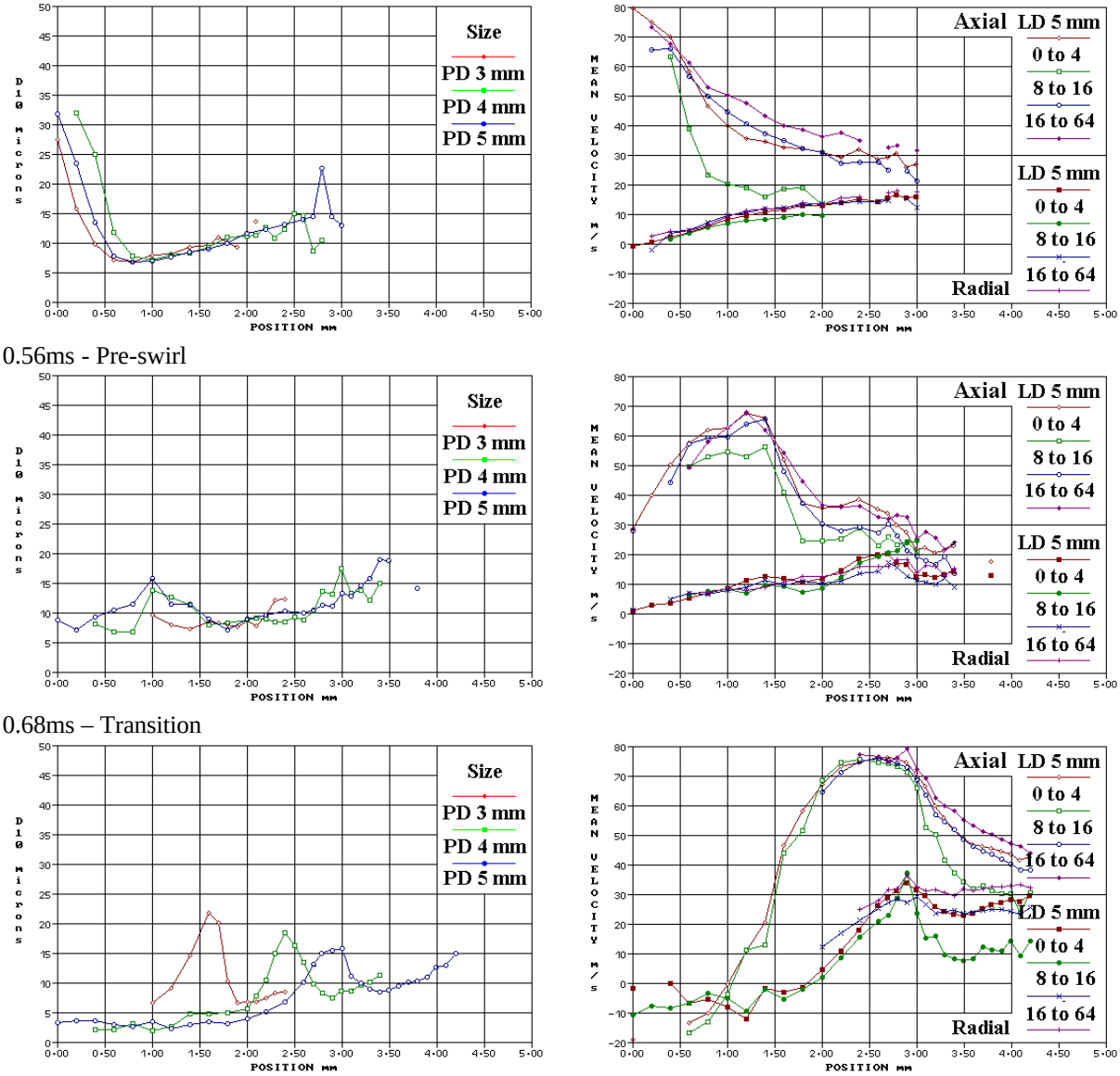

0.56ms - Pre-swirl

0.68ms – Transition

1.20ms – Fully developed cone

Figure 4 Dropsize,D_{10} and LD and PD velocity profiles as a function of dropsize class

The axial velocity profiles for the pre-swirl spray exhibit consistent high velocities, of up to 80 m/s, along the spray axis but strong gradients appear in the outer surface of the spray core as a function of size-class. For R = 1.0 mm the velocity gradient between the smallest and largest size class is 30 m/s. This radial position correlates with the minima in the recorded mean droplet diameters. It is also the location for which the radial velocity components show gradients in the velocity size-class profiles although the differences are small.

During the transition phase of the spray the axial velocity profiles exhibit strong size-class gradients across the whole radial profile. However, the velocity gradient between the smallest and largest size-classes has decreased, to 15 m/s. It is noted, that at this time, there is an exception to the general agreement between the LD velocity data and the profiles for the 8 to 16 micron size-class as there is a better correlation with the size-class 16 to 64 microns. As regards the velocity-size gradients in the radial velocity components then, again, they start from R = 1.0 mm and grow to over 10 m/s in the spray periphery.

For the fully developed spray cone phase at, 1.20 ms, the recirculation zone inside the hollow cone and the high peak velocities of the cone itself are readily identified. Only droplets of the smallest size-class 0 to 4 microns are to be found inside the hollow spray cone.

The dropsize profile for Z = 5 mm also shows that the mean D_{10} diameter is approximately 4 microns, from the spray axis out to R = 2.0 mm. Furthermore, very little gradient exists between this dropsize class and the LD velocity for both the axial and radial velocity profiles. This is to be expected, only the smallest droplets can be trapped inside the recirculation and they have a good flow tracking fidelity.

The mean droplet diameter profiles show peaks at nominally 22, 18 and 16 microns at radial positions R = 1.6, 2.4 and 2.9 mm respectively for the planes Z = 3,4 and 5 mm. These positions also indicate the start of the gradients in the axial velocity-size class profiles and the peak in the radial velocity-size class profiles. The velocity profiles shown, for the plane Z = 5mm in Figure 4, also indicate that the peak in the axial velocity profiles does not occur at the position R = 2.9 mm but before this, at R = 2.5 mm. The inference is that this is the radial location occupied by the high velocity remnants of the disintegrating liquid sheet. The radial location of the outer limit of the liquid sheet and for droplet generation, i.e. atomization, to reach a maximum can be inferred from the location of the peaks in the radial velocity profiles. With a strong velocity – size correlation, the larger size-classes maintain their high radial velocity out into the spray periphery as their flat radial profiles demonstrate. On the inside edge of the spray cone the radial velocity profiles also show a velocity – size correlation, unlike the axial velocity profiles. This is due to the low pressure region in the recirculation zone effecting all drop sizes in the range 0 to 16 microns.

The size class discrimination analysis is a powerful tool in interpreting the PD data but the sample number density must also be known to attach the correct weighting to the size-class data. This can be performed by plotting the sample number as a function of size as shown in Figure 5 for the point Z = 5 mm and R = 2.9 mm, the most optically dense part of the spray cone.

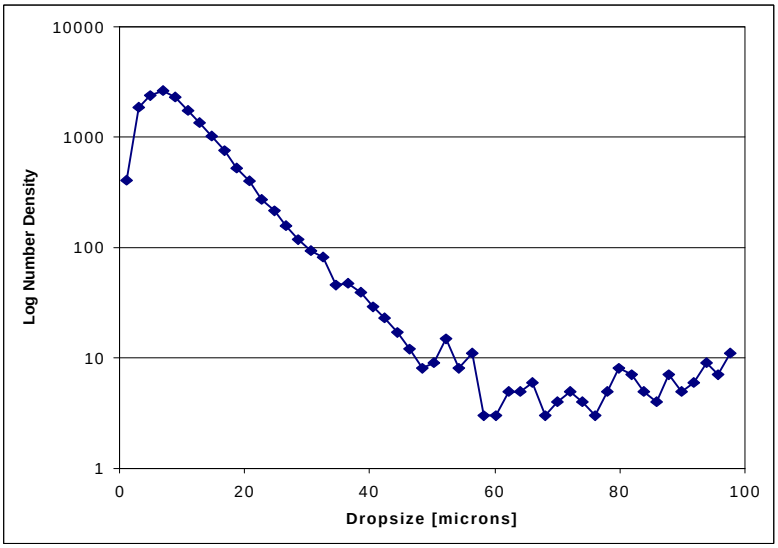

Figure 5 Sample number distribution according to dropsize class

The distribution is wide, the sizes recorded fill the instrumental measurement range. It suggests that there may well be droplets of a greater diameter than 100 microns present in the spray. This would agree with estimates of the maximum dropsize being equal to the annular fuel sheet thickness at the nozzle orifice which, for this injector, have been measured at between 0.12 to 0.15 mm, [8]. However, the number density of these large droplets is very low as 1000 injections were recorded at this measurement point.

4 Conclusions

The pre-swirl spray in this near nozzle region comprises of a pure jet flow but as the swirl momentum increases and the fuel is transferred radially outwards a low pressure zone on the spray axis is created. In the spray core the droplets are large and travel with the same velocity as the liquid fuel elements. This state changes when the droplets interact with the shear gradients generated in the spray periphery and by the transition from the pre-swirl to hollow cone. Strong shear gradients are set up between the different droplet size classes and the liquid fuel. The transition phase from pre-swirl to hollow cone is complete within 0.2 ms for this near nozzle region.

In the fully developed cone the low pressure region generates a recirculation zone which contains only droplets of the smallest size classes and LD and PD velocity are identical. The structure of the cone itself is inferred from:- (1) the peak in the axial velocity profiles indicates the radial location occupied by the high velocity remnants of the disintegrating liquid sheet and (2) the correlation between the peaks in the mean droplet diameter profiles and the peaks in the radial velocity-size class profiles indicates the radial location of the outer limit of the liquid sheet and the region where atomization is most effective. The droplet dynamics in the spray periphery are determined by a strong velocity – size correlation with the larger drop size classes maintaining their high radial velocity component and the smallest size classes influenced by the surrounding entrained air.

5 References

[1] Wigley, G., Heath J., Pitcher G. and Whybrew A., 2001 ‘Experimental Analysis of the Response of a Laser/Phase Doppler Anemometer to a Partially Atomized Spray’, *Part. Part. Syst. Charact*. Vol 18, pp 1 – 10

[2] Damaschke, N., Gouesbet, G., Grehan, G. Mignon, H., and Tropea, C., 1998 ‘Response of Phase Doppler Anemometer Systems to nonspherical droplets’, *Appied Optics*, Vol. 37, No. 10

[3] Allen, J. and Hargrave G., 2000 ‘Fundamental Study of In-Nozzle Fluid Flow and Turbulence and its Effects on Liquid Breakup in Gasoline Direct Injectors’, *ILASS-Europe 2000*, Darmstadt

[4] Le Coz, J. F. and Hermant, L., 1999 ‘Visualisation of Sprays Generated by Direct Injection Gasoline Engines’, *ILASS-Europe ’99*, Toulouse

[5] Wigley, G. Hargrave, G. K. and Heath, J., 1999 ‘A High Power, High Resolution LDA/PDA System Applied to Gasoline Direct Injection Sprays’, *Part. Part. Syst. Charact.*, Vol. 1

[6] Wigley, G., Goodwin , M., Pitcher G. and Blondel, D., 2002, ‘Imaging and PDA Anaysis of a GDI Spray in the Near Nozzle Region’, *Eleventh International Symposium Application of Laser Techniques to Fluid Mechanics*, Lisbon

[7] Smallwood, G. J. and Gülder, Ö. L., 2000, ‘Views on the Structure of Transient Diesel Sprays,’ *Atomization and Sprays*, 10, pp. 355-386

[8] Allen, J. and Hargrave G., 2003 ‘Investigation of Internal Flow in Real Sized Pressure Swirl Gasoline Direct Injectors’, *IMechE Conference Transactions 2003-2, Fuel Injection Systems,* ISBN 1 86058 399 7